

# Intercalibration of the DØ calorimeter

DØ internal Note

Pierre-Antoine Delsart, Julien Donini, Patrice Lebrun

12 Novembre 2003

**Abstract**

# 1 Principles and methods of the $\phi$ intercalibration

## 1.1 introduction

In order to have the best precision possible on the measurements of the calorimeter (energy and position of the electromagnetic particles, jets and missing transverse energy), several steps are necessary to calibrate the detector. The energy measured by the calorimeter is a convolution of the signal given by each cell, the energy scale fixed by the electronic calibration system and a set of correction factors such as non-linearity and gain calibration corrections (which provide the linearity between the energy deposited and the energy measured) and the geometrical effects corrections.

To improve the calibration precision of the detector it is in principle possible to make use of the  $\phi$ -symmetry of event activity, which should be the same for all cells in one floor at the same pseudorapidity ( $\eta$ ). By comparing the energy deposited in each cell for a ring at a fixed  $\eta$  with an energy of reference it is possible to perform a channel to channel local calibration of this ring, referred to as intercalibration.

## 1.2 Intercalibration procedure

### General methods

A simple method to intercalibrate a constant  $\eta$  ring of cells is performed by comparing the number of events exceeding a given energy threshold in each cell with a number taken as a reference. If  $f(E)$  is the distribution of the number of events as a function of the energy recorded in a unit of reference (for instance all the cells in one ring), then the number of events  $N(E_s)$  recorded above an energy threshold  $E_s$  is:

$$N(E_s) = \int_{E_s}^{\infty} f(E)dE \quad (1)$$

Let's now consider a cell in the same  $\eta$  ring (and layer) and suppose that the energy  $E'$  measured in this cell is related to the energy  $E$  measured in the reference unit by an intercalibration constant  $\alpha_i$ . In the most general case we have  $E' = \alpha_i E + \beta_i$ , however in our studies we will first consider that the contributions of the  $\beta$  constants are negligible. The distribution of recorded events  $g$  in the cell we want to calibrate is such as  $g(E')dE' = f(E)dE$  and we have the following relationship:

$$N_i(E_i) = \int_{E_i}^{\infty} g(E')dE' = \int_{E_s}^{\infty} f(E)dE = N(E_s) \implies E_i = \alpha_i E_s \quad (2)$$

where  $N_i(E_i)$  is the number of events above the energy threshold  $E_i$  in the cell we want to intercalibrate. In practice the intercalibration constant is obtained by calculating  $N(E_s)$  in the unit of reference and then by choosing  $E_i$  so as to have  $N_i(E_i) = N(E_s)$ . This algorithm will be referred to as the "N method".

Another way to calculate  $\alpha_i$  is to compare the energy sum of all the recorded events that pass the energy threshold to a sum of reference. The energy sum above the threshold  $E_s$  is defined by:

$$S(E) = \int_{E_s}^{\infty} E f(E)dE. \quad (3)$$

The intercalibration constant  $\alpha_i$  is then extracted when a threshold  $E_i$  is found such as  $S_i(E_i)/S(E_s) = E_i/E_s$  (this procedure is called “E method”).

To evaluate the intercalibration efficiency of these methods we simulated a virtual ring of 64 cells, each containing a random exponential distribution of energy miscalibrated by a known constant. Then we applied the two methods to reconstruct the intercalibration coefficients. The precision of each algorithm is given by calculating the standard deviation of  $(1 - \alpha_{rec}/\alpha_{generated})$  for the 64 cells. Figure 1 shows the resolution in the reconstructed constants as a function of the energy threshold  $E_s$  used. A third method (“mean E”), where the intercalibration factor is calculated by taking the ratio between the mean energy measured above a threshold and the mean obtained in the reference unit, is also shown. The first two methods (N and E) give better results and seem more appropriate in particular for high energies.

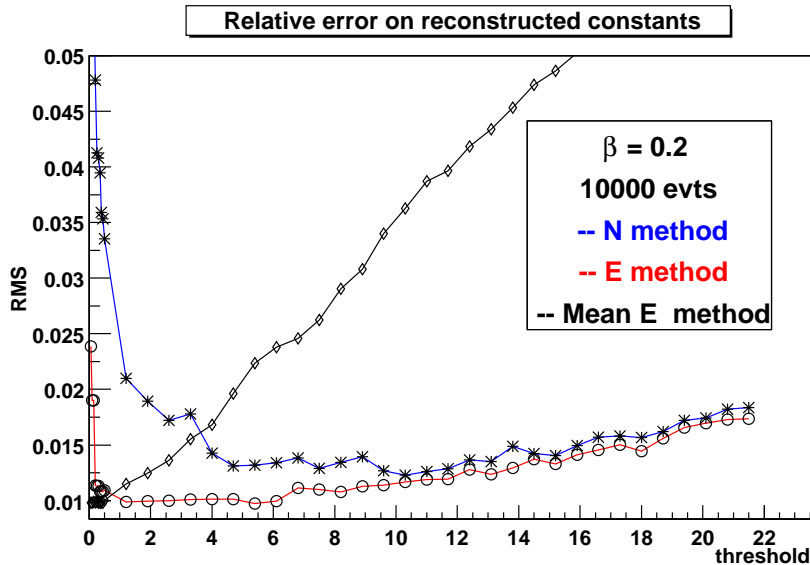


Figure 1: Precision of the reconstructed intercalibration constants as a function of the reference energy threshold, in GeV, for three different algorithm: “N” method (stars), “E” method (circles) and “mean E” (lozenges).

The influence of these intercalibration procedures on the energy flow in one ring of the calorimeter is shown in figure 2. The standard deviation of the energy flow is significantly reduced by the computation of intercalibration constants. This study was performed on the first sets of data available, however for some samples the intercalibration algorithm failed to reduce the standard deviation in the energy flow. Therefore a more general method was conceived where non zero  $\beta$  constants were considered. The relationship (2) then becomes:

$$N_i(E_i) = N(E_s) \implies \begin{cases} E_i = \alpha_i E_s + \beta_i \\ S_i(E_i) = \alpha_i S(E_s) + N(E_s)\beta_i \end{cases} \quad (4)$$

with the following parameters:

$$\alpha_i = \frac{E_i N_i(E_i) - S_i(E_i)}{E_s N(E_s) - S(E_s)} \quad \beta_i = E_i - \alpha_i E_s. \quad (5)$$

Simulation studies showed that this last method gives significantly better results on the resolution of the constant  $\alpha$  and the standard deviation of the energy flow than the other more simple methods described previously.

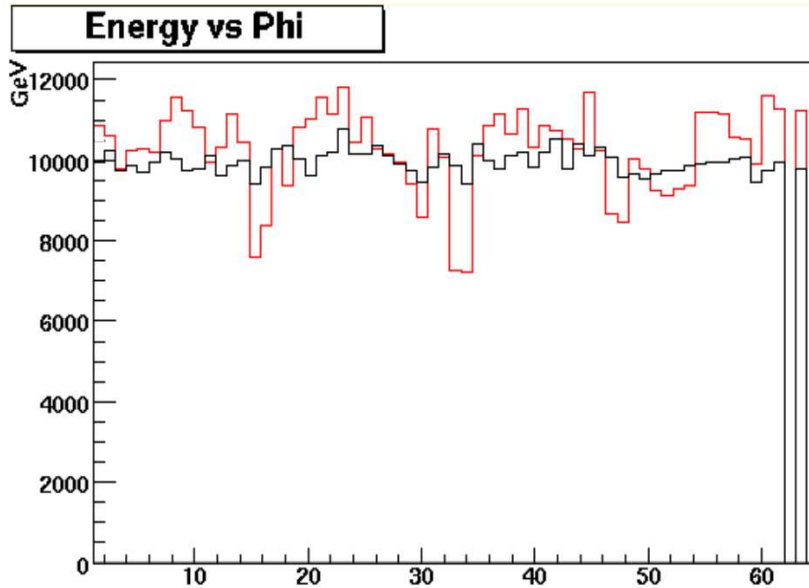


Figure 2: Energy flow in one ring of the calorimeter before (gray curve) and after (black curve) intercalibration for the first datasets studied.

### Selected methods

The intercalibration methods based on the flow of events give in theory very good results but they become inefficient if the flow of recorded events is not symmetrical in  $\phi$ . This can happen in particular in case of non-uniformities in the trigger system: the event rate is affected and the method will give biased results. However the method based on the mean energy measured above a threshold is less sensitive to trigger effects. Therefore two new intercalibration procedures were implemented combining the concepts developed in the previous methods:

- Method 1: the following value is calculated for each energy distribution in the cells we want to intercalibrate,

$$M_i(E_s) - \frac{N_{ref}(E_s)}{N_i(E_s)} E_s \quad (6)$$

where  $M_i(E_s)$  is the mean of the energies recorded above the threshold  $E_s$  in the  $i^{th}$  cell (the threshold  $E_s$  is the same for all cells in the  $\phi$  ring). This quantity is determined for  $n$  different thresholds  $E_s$  separated by an energy step  $e$  ( $e \sim E_s/20$ ). The same values are calculated for the unit of reference. The relationship between the mean values is  $M_i(E_s) = \alpha_i M_{ref}(E_s) + \epsilon(\alpha_i)$ , where  $\epsilon(\alpha_i)$  is a term that takes into account the threshold effect that appears when calculating the energy means. This effect is compensated by introducing the term  $N_{ref}(E_s)/N_i(E_s)$  in our equation. A linear fit is then performed

between the resulting values and the quantities calculated for the reference, which gives an approximation of the intercalibration constant  $\alpha_i$ . This process is reiterated once using the constant  $\alpha_i$  in the calculations to increase the precision on the intercalibration constant.

- Method 2: this second intercalibration procedure improves the method described in (4),

$$M_i(E_i) = \alpha_i M(E_s) + \implies E_i = \alpha_i E_s. \quad (7)$$

For each cell, to unscramble the intercalibration constant, an energy threshold  $E_i$  is searched such as

$$\frac{M_i(E_i)}{M(E_s)} - \frac{E_i}{E_s} = 0. \quad (8)$$

This method is independent of threshold effects and it can also be easily improved to take into account the  $\beta$  constants.

These last two methods present several advantages compared to the more general methods described previously. They are less sensitive to trigger effects, their efficiency is good at high energy (the resolution on the intercalibration constants is optimal for energy threshold above 2 GeV) and the calculation of  $\alpha$  constants is not affected by possible offset effects (such as pedestal fluctuations). For all these reasons those intercalibration procedures have been selected and were applied on  $D\bar{O}$  data.

The performance of each method was tested on a virtual ring generated from real data recorded in the first layer the calorimeter. The energy measured in each cell was miscalibrated by a set of generated constants and then the methods were applied. The precision in the reconstruction of the intercalibration constants is measured by the standard deviation of the  $(1 - \alpha_{rec}/\alpha_{gen})$  distribution. Figure 3 shows the precision of each method as a function of the miscalibration constant generated (the statistics correspond to 3.8 millions events).

## 2 Simulation of the intercalibration

In order to understand the impact of intercalibration constants on the measured energy we have performed a study of the Z boson width based on Monte-Carlo events. The idea is to see to what extent the application of the sole intercalibration procedure on the calorimeter can improve the energy resolution on reconstructed events.

### 2.1 Expected effects on the energy resolution

The total energy deposited by an electron in the calorimeter can be written:

$$E_{\text{Total}}^2 = \sum_i E_i^2 + 2 \sum_{i<j} E_i E_j \quad (9)$$

with  $E_i$  is the energy deposited in the  $i^{\text{th}}$  cell. We suppose that the energy measured in one cell can be expressed as:

$$E_{\text{measured}} = \alpha E' \quad (10)$$

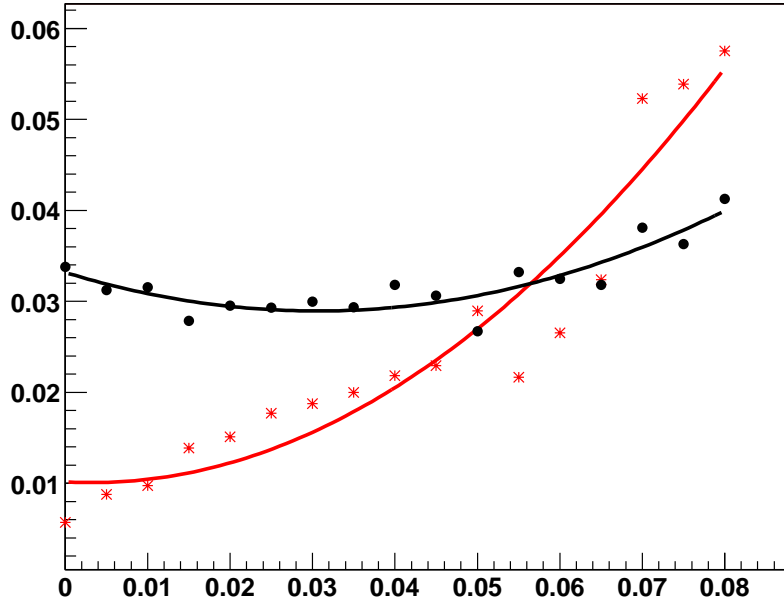


Figure 3: Precision of the two final intercalibration methods as a function of the miscalibration applied on the data. The gray curve (stars) corresponds to the first selected method and the black curve (dots) to the second method.

where  $E'$  is the individual response of the cell for a deposited energy  $E$  and  $\alpha$  is the relative miscalibration constant with respect to the other cells in the ring. Then the deviation of the measured energy from the real deposited energy will be the mean of the following value:

$$\begin{aligned}
 (E_{\text{Tot measured}} - E_{\text{Tot real}})^2 = & \sum_i \alpha_i^2 (E'_i)^2 + \sum_i \alpha_i^2 E_i^2 - 2 \sum_i \sum_j \alpha_i E'_i E_j \\
 & + 2 \sum_{i < j} (\alpha_i \alpha_j E'_i E'_j) + 2 \sum_{i < j} E_i E_j
 \end{aligned} \tag{11}$$

If we separate the factors  $\alpha^2$  in  $(\alpha^2 - 1) + 1$  and if we take the average on a large number of events, we obtain:

$$\begin{aligned}
 \sigma^2 = & \sum_i [(\alpha_i^2 - 1) \overline{E_i'^2}] + 2 \sum_{i < j} (\alpha_i \alpha_j - 1) \overline{E'_i E'_j} \\
 & - 2 \sum_i \sum_j (\alpha_i - 1) \overline{E'_i E_j} + \sigma_{\text{calibrated}}^2
 \end{aligned} \tag{12}$$

The “ $\sigma_{\text{calibrated}}$ ” term in this equation contains all effects other than the miscalibration and corresponds to the resolution of a perfectly calibrated detector. Then by considering the mean on the  $\phi$  position of the particle, we obtain:

$$\begin{aligned}
 \langle \alpha_i \alpha_j - 1 \rangle &= 0 \\
 \langle \alpha_i - 1 \rangle &= 0 \\
 \langle \alpha_i^2 - 1 \rangle &= \sigma_{\text{misc}}^2
 \end{aligned} \tag{13}$$

If we suppose that the calorimeter is uniformly miscalibrated, the term  $\sigma_{\text{misc}}$  is a constant and we have:

$$\sigma^2 = \sigma_{\text{misc}}^2 \left( \sum_i \overline{E_i'^2} \right) + \sigma_{\text{calibrated}}^2. \quad (14)$$

Moreover the term  $\overline{E_i'^2}$  can be expressed as

$$\overline{E_i'^2} = \bar{E}_i^2 + \sigma_{\text{cell}}^2 \quad (15)$$

where  $\sigma_{\text{cell}}$  represents the errors on the energy of the cell other than those coming from the miscalibration. Finally if we make the gross estimation that  $\sum \bar{E}_i^2 \sim E_{\text{Total}}^2/n$ , where  $n$  is the number of cells in the cluster, we obtain:

$$\boxed{\frac{\sigma}{E} = \sqrt{\frac{1}{n} + \frac{\sigma_{\text{cell}}^2 n}{E^2}} \sigma_{\text{misc}} \oplus \frac{\sigma_{\text{calibrated}}}{E}} \quad (16)$$

In order to evaluate the effect of the intercalibration we performed a similar calculation using corrected constants  $\alpha'$ . These constants are corrected with respect to a mean constant in a given  $\eta$  ring. Thus if we write  $(\alpha_i'^2 - 1) = (\alpha_i'^2 - \alpha_\eta^2) + (\alpha_\eta^2 - 1)$ , the mean on the  $\phi$  position becomes:

$$\langle \alpha_i'^2 - 1 \rangle = \sigma_{IC}^2 + (\alpha_\eta^2 - 1) \quad (17)$$

where  $\sigma_{IC}$  is the precision of the intercalibration method. We can also estimate that  $(\alpha_\eta^2 - 1) \sim \sigma_{\text{misc}}^2/64$ , which gives:

$$\boxed{\frac{\sigma}{E} = \sqrt{\frac{1}{n} + \frac{\sigma_{\text{cell}}^2 n}{E^2}} (\sigma_{\text{misc}}/8 \oplus \sigma_{IC}) \oplus \frac{\sigma_{\text{calibrated}}}{E}} \quad (18)$$

We see that the intercalibration can improve the energy resolution if the precision on the intercalibration constants is high enough:

$$\sigma_{IC} < \frac{\sqrt{63}}{8} \sigma_{\text{misc}}. \quad (19)$$

## 2.2 Simulation of the intercalibration on Monte Carlo data

The energy resolution of the calorimeter has a direct influence on the measured width of the  $Z^0$  invariant mass peak. Therefore we tried to test the previous calculations by simulating the miscalibration and the intercalibration on Monte-Carlo events.

A complete Monte-Carlo study of intercalibration effects would have implied to generate millions of events in order to obtain enough statistics to use the previously described algorithm and calculate intercalibration constants for all cells in the calorimeter. Then we would have applied these correction factors on miscalibrated  $Z \rightarrow e^+e^-$  events and measured the impact of intercalibration corrections on the energy resolution. The first step of this procedure was however impossible to perform because of the very large CPU power and time needed to generate such an amount of events.

Therefore we preferred to work directly on a batch of  $Z \rightarrow e^+e^-$  events simulated with PYTHIA and reconstructed with the p11.13 version of d0reco. The method used is the following: for a given miscalibration hypothesis, we associate to each cell of the calorimeter a coefficient  $(1 + \epsilon_i^M)$  generated from a gaussian distribution of mean  $\mu = 1$  and variance  $\sigma_{Misc}^2$ . Next we calculate for every ring of cells a *reference* value

$$(1 + \epsilon_{\text{ref}}) = \sum_i \frac{(1 + \epsilon_i^M)}{N}, \quad (20)$$

where  $N$  is the number of cells in a  $\phi$  ring. The *true* intercalibration factor that should be applied to each cell is then:

$$\alpha_i = \frac{1 + \epsilon_{\text{ref}}}{1 + \epsilon_i^M}. \quad (21)$$

We suppose that this constant  $\alpha_i$  is known with a precision  $\sigma_{IC}$ . We generate a gaussian distribution of constants  $(1 + \epsilon_i^{IC})$  and calculate for each cell an intercalibration coefficient

$$\alpha_i^{IC} = \alpha_i \times (1 + \epsilon_i^{IC}) \quad (22)$$

that we will apply to the data.

In practice we generate two sets of constants  $\epsilon_i^M$  and  $\epsilon_i^{IC}$  and then for each event we do the following sequence of operations:

- miscalibration of the energy reconstructed in a EM cluster;
- non-linearity corrections<sup>1</sup> and intercalibration corrections for each cell of the cluster;
- geometrical corrections of the cluster energy.

Then we select the electrons that pass the official EM ID certification cut, that are not in the dead sectors of the calorimeter and with a transverse energy higher than 25 GeV. The Z invariant mass is reconstructed from the two highest energy electrons.

The same batch of events (corresponding to 890 selected Z events) was reprocessed with a relative miscalibration  $\sigma_{Misc}$  ranging from 1% to 10% and a precision  $\sigma_{IC}$  on the intercalibration constants between 0.5% and 10%.

The figure 4 shows the effective width<sup>2</sup> of the reconstructed Z invariant mass peak as a function of the miscalibration applied to the calorimeter. For instance for a miscalibration of 6% the effective width of the Z peak increases by about 12%.

The next two figures (5 and ??) show the effects of the intercalibration on the effective width of the Z mass peak for two different miscalibration hypothesis (respectively 2% and 7%). We observe that for each curve there is a precision on the intercalibration constants under which the Z sigma width is improved (dashed line). This limit also increases with the miscalibration value.

The intercalibration precision required to improve the results on the Z mass is shown as a function of the miscalibration in figure 6. This confirms that the sole application of the intercalibration can improve the energy resolution but also that a bad precision in the intercalibration constants will have the opposite effect.

<sup>1</sup>The code used for the non-linearity and geometrical corrections comes from the “em\_utils” routine.

<sup>2</sup>The effective width corresponds to the interval  $[M_0 - \sigma, M_0 + \sigma]$  around the Z invariant mass peak  $M_0$  containing 68% of the events in a 70 - 110 GeV window.

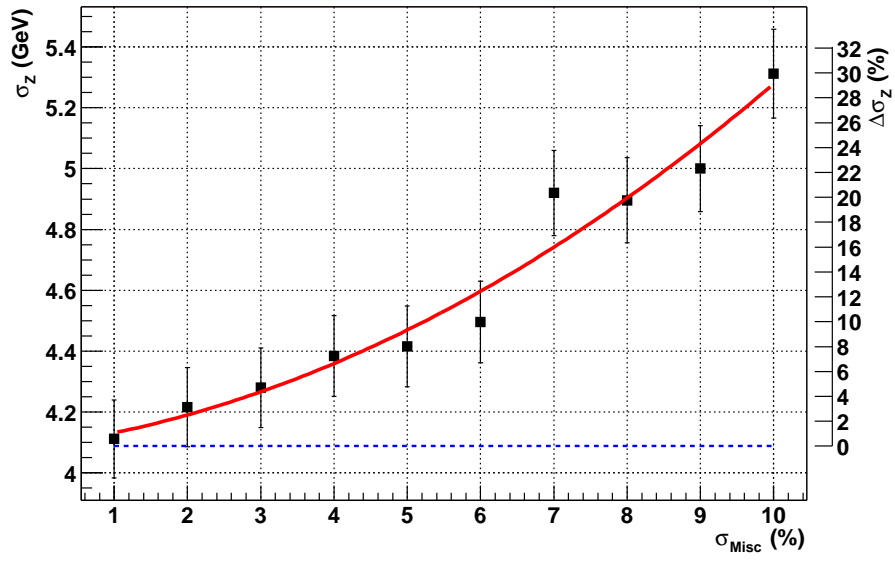
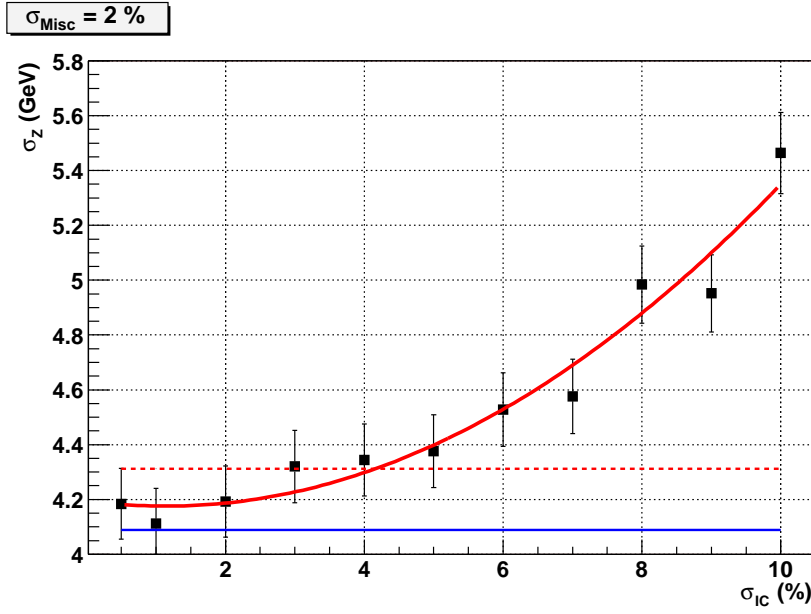
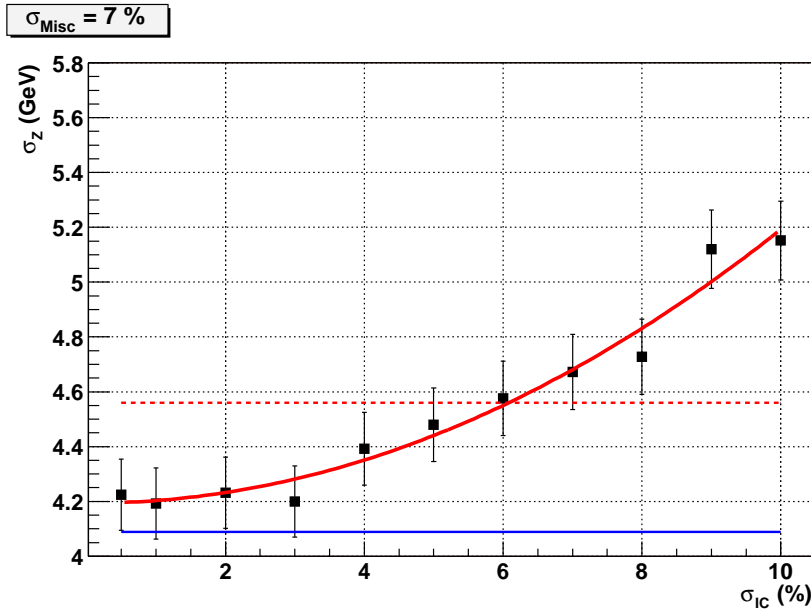


Figure 4: Width of the Z invariant mass peak (effective sigma) as a function of the miscalibration of the calorimeter. The horizontal line corresponds the Z peak width obtained without miscalibration.



(a)



(b)

Figure 5: Effective sigma of the reconstructed Z, after intercalibration, as a function of the precision on the intercalibration constants  $\sigma_{IC}$  and for two given miscalibration of the detector: (a)  $\sigma_{Misc} = 2\%$ , (b)  $\sigma_{Misc} = 7\%$ . The Z sigma width when no miscalibration is applied (continuous line) or after miscalibration but without intercalibration (dashed line) is shown as well.

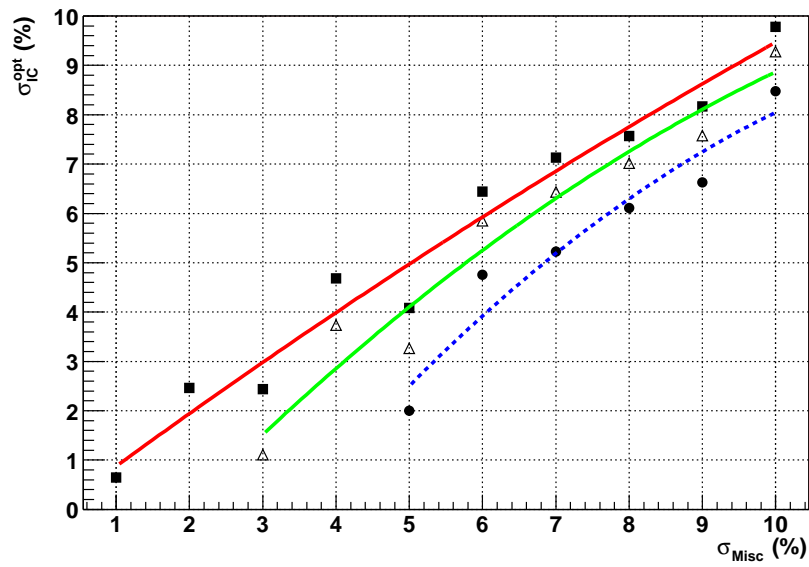


Figure 6: Required precision on the intercalibration constants to improve the Z mass width, as a function of the miscalibration. Black curve (squares), the effective sigma width is reduced by 0%, gray curve (triangles): 2%, dotted line (circles): 5%.

## 3 Data selection and acquisition

### 3.1 Storing calorimeter information

As  $\phi$  intercalibration is a statistical calibration, we need considerable amounts of information to ensure a good reconstruction of calibration constants. For a precision of reconstruction of  $\sim 1\%$ , information from  $\sim 10$  millions events is needed. It is far too long to reanalyze such a number of events directly from TMB files each time we need to calculate a set of constants. We thus developed our own computing tools in order to be able to store and access easily all this information. We have associated each cell with one histogram which stores the energy of the hits recorded by the cell. Each histogram is associated to a “virtual cell” (ICVirtualCell) which are grouped into “virtual layer” (IClayer), in correspondence with the real cells and layers of the calorimeter. We have defined some calibration zone (ICUnit) which can have any desired size and which are associated to a couple  $(\alpha, \beta)$  of calibration constants. These calibration units are grouped in a “virtual ring” (ICRing) which is the reference for the calibration of its ICUnits. More information and technical details can be found in annex A.1

### 3.2 Data quality control

The bad behavior of some cells of the calorimeter may introduce bias in the calibration algorithms. We have thus different procedures to avoid them.

First we ignore all hits below 200 MeV. Then we ignore hot cells that have been identified by NADA algorithm. Finally we need to remove noisy or dead cells. This can not be done on event by event basis and we do it on a run by run basis using the following simple procedure. After having recorded data from one run (or more than  $\sim 150\,000$  events) we consider each calorimeter ring and flag as bad all cell that do NOT enter the interval

$$\frac{1}{1.3}N_{med} < N_{cell} < 1.3N_{med} \quad \text{and} \quad \frac{1}{1.3}E_{med} < E_{cell} < 1.3E_{med} \quad (23)$$

where  $N_{med}$  and  $E_{med}$  are the medians value in the ring for total number of hits in cell and total energy recorded in cell. Bad cells are ignored, a map of bad cell is generated and the number of events in the corresponding run is saved. This allows us to scale distribution in cells in order to calibrate cells that had a bad behavior during some runs and good during other runs.

In some early data we also noticed that energy distribution in some cells had strange peak between 10 and 20 GeV. This peaks were preventing calibration algorithms to work. We thus added some tests at calibration time to detect such peak and set some high threshold in the algorithms to exclude the peaks.

### 3.3 Level 1 trigger selection

An important bias for intercalibration comes from the trigger level 1. For example, several calorimeter tower trigger were off or had a very low rate during the runs used for intercalibration. We applied an event selection based on L1 trigger such that in the final set of events the trigger distribution are  $\phi$ -uniform. This reduces non-uniformities in the calorimeter datas

and, as calorimeter electronic is different from trigger electronic, we should have low correlation between trigger effects and miscalibration effects. More details on this selection can be found in annex A.1.

This selection does not eliminate the problem of non-working trigger towers. It produces rings of uniform trigger towers with eventually one or two bad towers. Energy distributions are biased in the region corresponding to these towers and we thus flag as bad the corresponding cells. We eliminate a  $4 \times 4$  ( $8 \times 8$ ) zone of cells in the EM (HAD) calorimeter for each bad tower. Due to the large number of bad trigger tower only  $\sim 60\%$  of the calorimeter could be calibrated.

An other selection that we did not have time to implement would be based on EM candidate or jet distribution in the calorimeter. Instead of imposing a  $\phi$  symmetric trigger tower distribution one could impose a symmetric distribution of reconstructed object. This would provide a trigger independent selection of  $\phi$  symmetric set of data.

## 4 Results on data

We have calculated several sets of intercalibration constants from the data available. The results presented in this section were produced from a sample of 3.8 millions events that passed our trigger selection and that were reconstructed with the p11.11 version of d0reco.

### 4.1 Evaluation of the calorimeter miscalibration and the intercalibration precision

In order to estimate the relative miscalibration of the calorimeter we have compared the mean energy deposited in each cell. If the energy distribution in one cell has a variance  $\sigma^2$ , then the error on the mean energy in a ring should be  $\sim \frac{\sigma}{\sqrt{N}}$ , with N the mean number of events registered per cell. A larger standard error shows the miscalibration between the cells in the ring. The global energy distribution taken from the data is used to generate several virtual rings in which the miscalibration is simulated. We estimate the miscalibration of the calorimeter rings by searching the miscalibration hypothesis that fits better to the mean standard deviation of the data. Using this procedure and supposing that the miscalibration is uniform we estimate that the standard deviation of  $\alpha$  constants is higher than 4% (see figure 7).

Once the miscalibration of the calorimeter is estimated we can calculate the precision that the intercalibration procedures can reach in the reconstruction of the constants. First we estimate the miscalibration of each ring and then we simulate virtual rings, according to these miscalibration values, on which we apply the intercalibration procedures selected previously (methods “1” and “2”). The results are shown in figure 8: the precision obtained goes between 1% and 2.5% in average, except for some central rings ( $i\eta = -1, -2, -3$ ) where the estimated miscalibration is higher. In most cases the calculated precision on intercalibration constants is much better than the estimated miscalibration. Therefore, according to figure 6, we expect intercalibration procedures to have a positive effect on the calorimeter energy resolution.

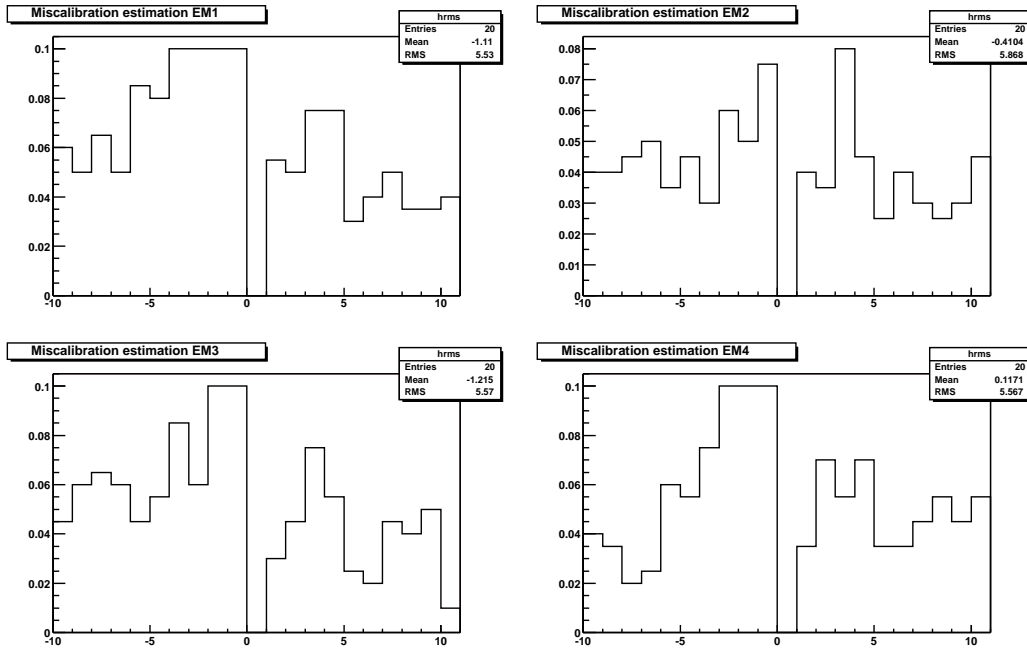


Figure 7: Estimation of the miscalibration of  $\eta$  rings in the central calorimeter.

## 4.2 Results

Intercalibration constants, when applied to the data, must in principle uniformize the energy distribution in the rings. As we can observe in figure 9 the standard deviation of the mean energy recorded in the cells is reduced after intercalibration. This however is not significant since constants reconstructed with a poor precision can also reduce the standard deviation. Therefore in order to test the intercalibration procedures we have applied the calculated constants to a batch of  $Z \rightarrow e^+e^-$  events and measured their effect on the  $Z$  reconstructed invariant mass peak.

The studied events have been taken from the “two electromagnetic particles” selection of the collaboration for the p13.05 and p13.06 reconstruction version. These data correspond to approximately  $72 \text{ pb}^{-1}$ . The following cuts have been applied:

- official em-id cuts on electrons;
- track matching for each particle (the angles are calculated from the tracks and are independent of the energy measured in the calorimeter);
- $\phi$  angle of the two particles in  $[\pi - 0.2, \pi + 0.2]$ ;
- no energy deposition in dead parts of the calorimeter;
- two particles in the barrel;
- $E_T > 20 \text{ GeV}$ .

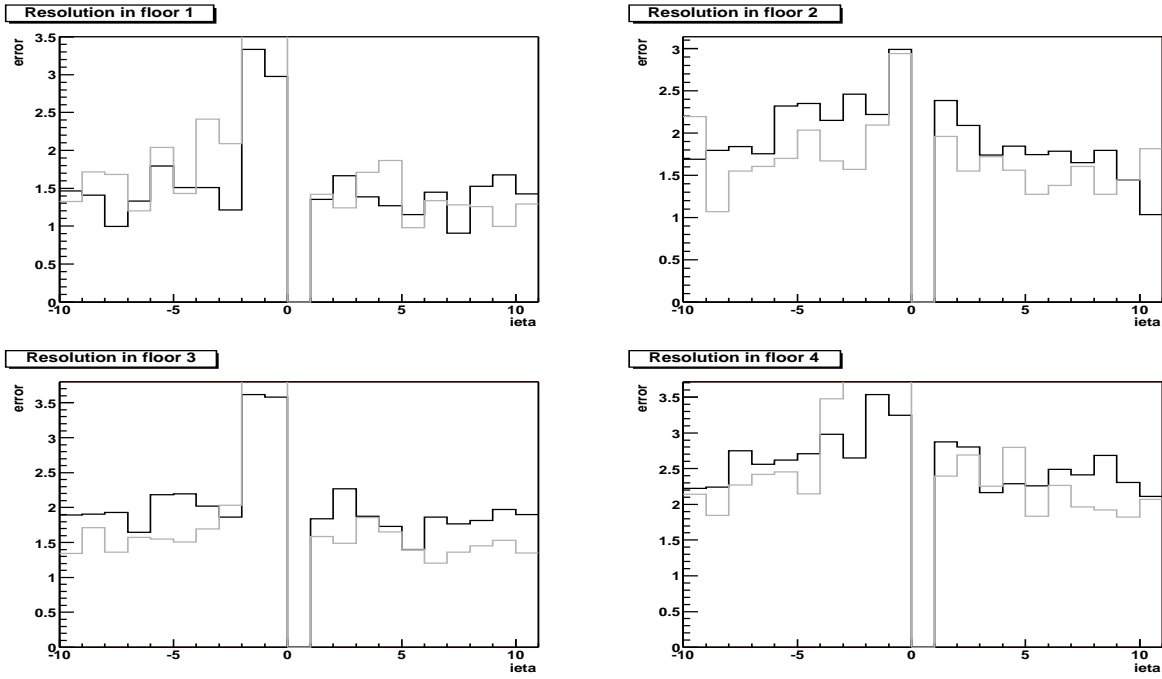


Figure 8: Precision of each intercalibration method in the barrel (gray: method 1, black: method 2).

The reconstructed invariant mass peak is fitted with a Breit-Wigner function convoluted with a gaussian. The two free parameters of the fit are the width of the gaussian function and the mean of the Breit-Wigner function, the width of the Breit-Wigner being fixed to 2.49 GeV.

Intercalibration constants have been calculated for all calorimeter cells from events selected in the p11.11 reconstruction version. We did not use the p13 versions for technical reasons and lack of time. This should not have an impact in our study since the intercalibration is a calibration of lower level and it comes before most reconstruction algorithms. Moreover there are no difference in electronic corrections between the versions we used.

The effect of the two intercalibration methods on the width of the Z mass peak is shown in figures 10 and 11. The results obtained with the non-linearity and gain corrections and the geometrical corrections is also given as a comparison. We observe that the intercalibration methods do not seem to improve the width of the Z mass peak.

## 5 Conclusion

As for a conclusion about this work on phi intercalibration, there are two main points that we want to highlight.

First, a complete 'framework' has been set up and is ready to work. It is contained in the package `cal_phi_calib` and documented in the annex of this document. It defines storage structures, and procedures for selecting events, estimating miscalibration of the calorimeter and two optimized algorithms for calibration.

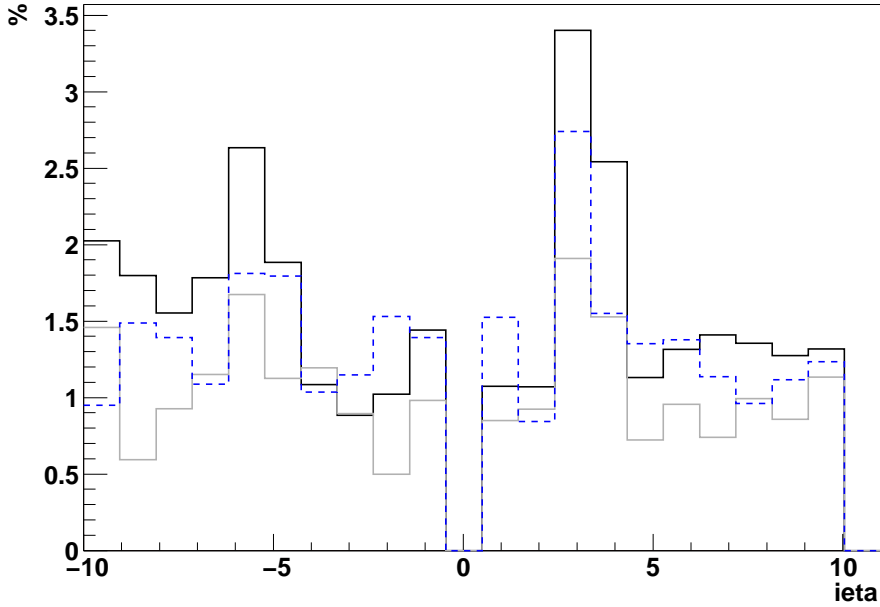


Figure 9: Standard deviation of the mean energy of all cells in a ring as a function of the ring position (in EM1). Black curve: no intercalibration, gray curve: method “1”, dashed line: method “2”.

Second, these procedures have been applied to calculate calibration constants on data from d0reco p11. We evaluated that the global miscalibration of the calorimeter was above 4% which does not correspond to a uniform calorimeter. The precision on the reconstruction of the constant was around 2%. Given this number and following our hypothesis, we expected a good improvement on the EM energy resolution. We had a test on di-electron sample from a completely independent set of events (d0reco p13) : although the intercalibration slightly reduced the width of the Z mass peak, it did not reach the significant expected improvement. We have three options to explain this :

- The event selection is not completely free of trigger bias and could be improved.
- As phi intercalibration is a statistical calibration, even small systematic effects (for example a default in electronic corrections) can spoil the reconstruction algorithms.
- A lot of default were not corrected on the data used to calculate the constants (“ring of fire”, “cross-talks”,...) and the resulting effects could completely dominates our corrections.

Now numerous improvement have been done on the data quality of the calorimeter. Phi intercalibration should perform better with good quality data and we recommend apply it on recent events. An other estimation of the global miscalibration would be very important and may confirm the necessity of phi intercalibration.

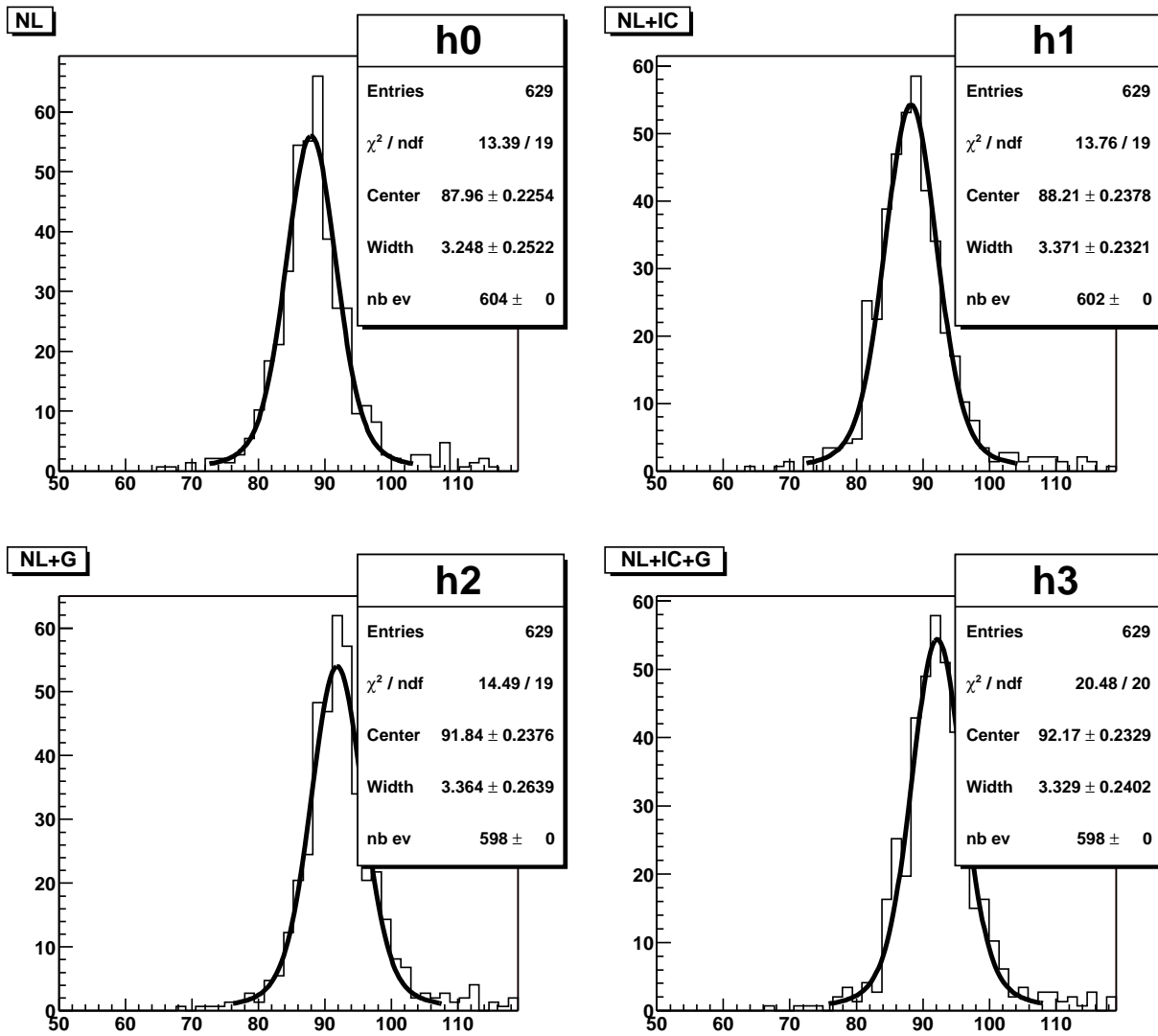


Figure 10: Z invariant mass reconstructed from the data for different types of corrections: non-linearity and gain (NL), geometrical (G) and intercalibration (IC) for method 1.

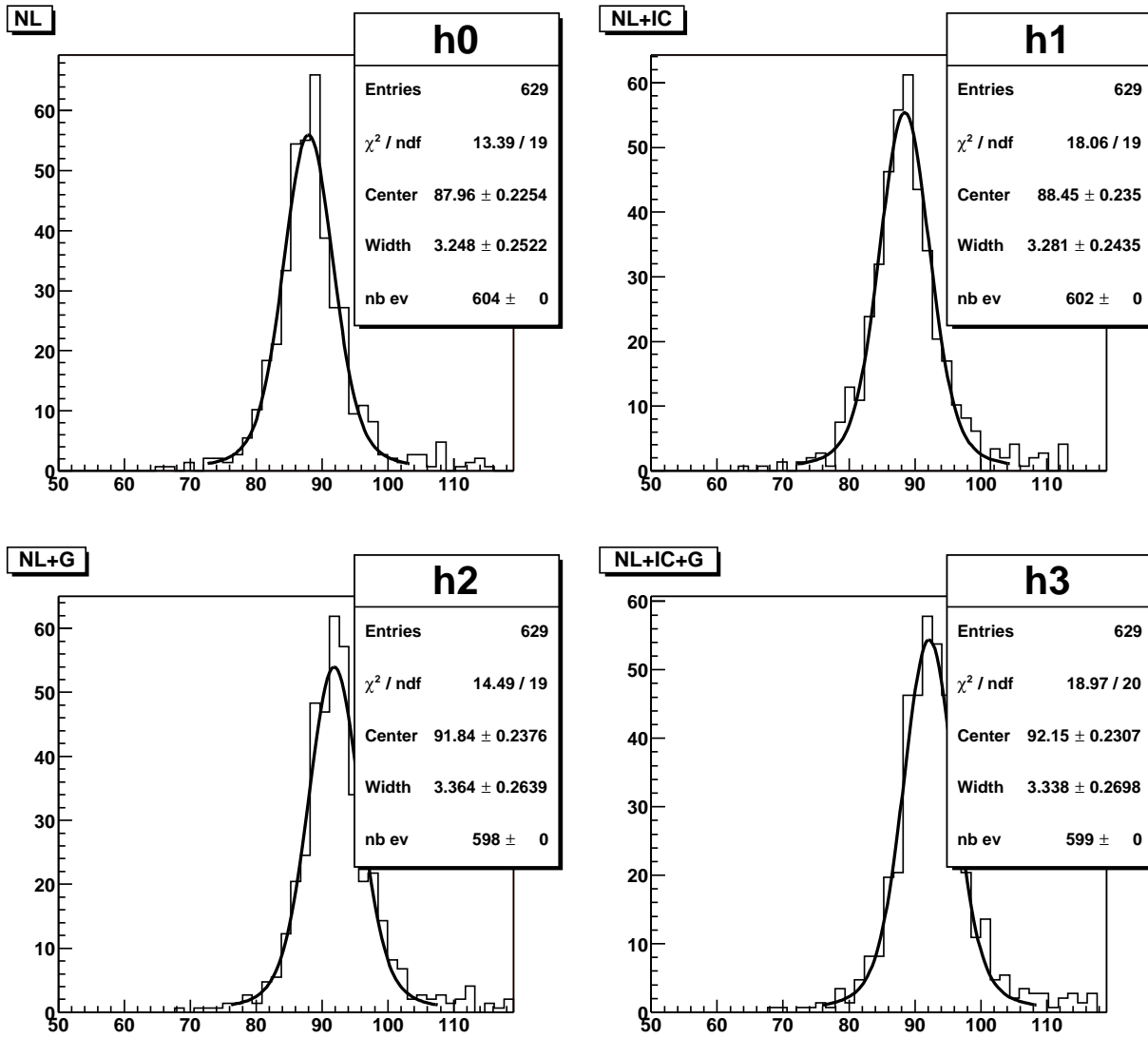


Figure 11: Same as figure 10 but for the second intercalibration procedure (“method 2”).

# A Intercalibration code

## A.1 Intercalibration classes

### A.1.1 Cell classes

The base class is **ICVirtualClass**. It is defined by a position in (ieta,iphi) indices, and a couple of miscalibration constant ( $\alpha, \beta$ ) for testing purpose. It has virtual functions for filling and unfilling the cell with energy hits and for getting global quantities such as energy flow and number of events between two thresholds. These functions are implemented in derived classes : we have implemented **ICHistBaseClass** where energy hits are stored in a histograms. This class does not specifies the histogram but only implements the virtual functions. The histogram is defined as a ROOT TH1 in the derived class **ICHistBiasClass** with appropriate binning.

### A.1.2 Layer class

The class **ICLayer** is designed to store cells as the real calorimeter layers. One can define the eta range of the ICLayer and the number of cells in a ring (default=64). ICLayer uses a TClonesArray of object inheriting from ICVirtualCell (we use ICHistBiasCell) and provide a Fill function to store energy hits to the ICVirtualCells it contains.

### A.1.3 Calibration zones

Calibration zone are defined by **ICUnit**. This class contains a ROOT TList whose elements are ICVirtualCells. This gives the possibility to associate a group of cells to one calibration zone. Each ICUnit also contains a couple of calibration constant which can be calculated with the 'Calibrate' function.

**ICListUnit** is derived from **ICUnit** and defines a list of calibration units. It is used to define the reference sample of the calibration algorithms.

**ICRing** provide a simple way to calibrate a ring of cell of the calorimeter. It is associated to a ICLayer and it links this ICLayer's ICVirtualCells to a list of ICUnits in a ICListUnit. It contains thus a ICListUnit that represents a ring at a given eta. It also contains a calibrator algorithm (ICStandardCalibrator, see below) and reference ICUnit (by default, this reference is simply the whole ICListUnit of cells). It provides a 'Calibrate' function that calls the 'Calibrate' function of all the ICUnits using the ICStandardCalibrator and the reference ICUnit. Finally it contains a list of bad cells to be ignored during the calibration procedure.

### A.1.4 Calibration algorithms

The calibration algorithms described previously are implemented in classes inheriting from **ICStandardCalibrator**. This base defines only two energy thresholds (low and high) and a virtual 'Calibrate' function which calculates a couple ( $\alpha, \beta$ ) of calibration constants for a ICUnit using a reference ICUnit.

**ICmethod1Calibrator** and **ICmethod2Calibrator** contains the algorithms described in section 1.2

### A.1.5 Utilities class

The **ICTools** class provides functions to easily manage ICLayer.

- Lots of drawing functions (such as energy flow, mean energy, number of hits vs  $\eta$  or  $\phi$ ).
- Procedure to detect bad cells and create maps of bad cells, and to merge the good cells of two layers.

## A.2 DØ framework executable

A framework executable is provided in the package `cal_phi_calib`. It is named **IClayermaker**, it reads the caldata chunk of a TMB file and outputs a root file containing a ICLayer. All options are described in the RCP file corresponding to this executable. This program does not implement the trigger selection (see A.3) but it takes in input a flat ascii files containing the list of event number to store in the ICLayer. Note that this list must be sorted and the first element must be the number of event in the list.

This executable is very simple and aims to use DØ framework only to get out calorimeter information. The remaining work such as finding bad cells, merging ICLayers and calculating the constants should be done with the others executables.

## A.3 Stand alone executables

These executables run outside DØ framework. The code source is provided in `cal_phi_calib` with the corresponding Makefiles. The executables must be linked with a shared library containing all intercalibration classes (a Makefile is also provided to compile this library).

### A.3.1 The trigger selection

The goal of the trigger selection is to reduce at best the bias coming from L1 trigger non-uniformities. For this we choose events such as the final set of events as  $\phi$  uniformity in the number of hits recorded by the trigger towers. This allows us to use all events that fired only a calorimeter trigger and thus maximizing statistics. This method solves the problem due to defective trigger tower that don't fire when they should but does not completely avoid bias coming from miscalibrated trigger tower.

The source code is in the `triggreescan.cxx` file. It is rather complex because L1 trigger bits may vary from one trigger configuration file to an other. It takes in input a small tree containing only relevant information (L1 bits, trigger simulation from data and NADA information, see file `triggtree.cxx`. Unfortunately this could not be ported to d0 framework but shouldn't be of any difficulties), and performs the following operations :

- It checks that trigsim output corresponds to the L1 output.
- It checks that no NADA cell was in any trigger tower.
- It counts number of hit in the trigger towers and measure mean energy

- It detects bad trigger tower with quality checks similar to those in equation (23).
- It performs the event selection excluding bad trigger towers and produces a map of cells corresponding to these towers.

Again because of technical details, this code is not very simple and an other selection based on EM object (as discuss in 3.3) would be much more simple to implement.

### A.3.2 Quality control

A very simple executable **ICBadchan.cxx** takes a ICLayer in input, creates a map of bad cells for this layer (using eq (23)), and merge its good cells to another one.

### A.3.3 Calibration procedure

Two executables **ICcalibLayer1** and **ICcalibLayer2** performs the calibration of one ICLayer using the intercalibration algorithms 1 and 2. Essentially, they compute best high and low energy thresholds and fine tune the intercalibration parameters using the energy distribution stored in the ICLayer. They output a flat ascii file listing calibration constants and estimated precision for each cells.